STUDY ON NANODOT OSLD IN AIR CAVITY USING 12 MeV ELECTRON BEAM RADIOTHERAPY

FARAHAMIZAH BINTI OTHMAN

SCHOOL OF HEALTH SCIENCE
UNIVERSITI SAINS MALAYSIA

2024

STUDY ON NANODOT OSLD IN AIR CAVITY USING 12 MeV ELECTRON BEAM RADIOTHERAPY

by

FARAHAMIZAH BINTI OTHMAN

Dissertation submitted in fulfilment of the requirements
for the degree of Bschelor of Health Science (Honours) (Medical Radiation)

JULY 2024

CERTIFICATE

This is to certify that the dissertation entitled "**STUDY ON NANODOT OSLD IN AIR CAVITY USING 12 MeV ELECTRON BEAM RADIOTHERAPY**" is the bona fide record of research work done by **FARAHAMIZAH BINTI OTHMAN** during the period from October 2023 to June 2024 under my supervision. I have read this dissertation and that in my opinion it conforms to acceptable standards of scholarly presentation and is fully adequate, in scope and quality, as a dissertation to be submitted in partial fulfilment for the degree of Bachelor of Health Science (Honours) (Medical Radiation).

Main Supervisor:

……………………………
Dr. Mohd Fahmi bin Mohd Yusof
Senior Lecturer
School of Health Sciences
Universiti Sains Malaysia
Health Campus
16150 Kubang Kerian
Kelantan, Malaysia

Co-Supervisor:

………………………………
Cik Arifah Nazirah binti Abdullah
Medical Physicist,
School of Health Sciences
Universiti Sains Malaysia
Health Campus
16150 Kubang Kerian
Kelantan, Malaysia

Field-Supervisor:

……………………………
Encik Ahmad Bazlie bin Abdul Kadir
Research Officer
Secondary Standard Dosimetry Laboratory (SSDL)
Radiation Metrology Group
Malaysian Nuclear Agency
43000 Bangi, Kajang
Selangor

Date: July 2024

DECLARATION

I, Farahamizah binti Othman hereby declare that the dissertation entitled "**STUDY ON NANODOT OSLD IN AIR CAVITY USING 12 MeV ELECTRON BEAM RADIOTHERAPY**" is the result of my own investigations, except where otherwise stated and duly acknowledged. I also declare that it has not been previously or concurrently submitted as a whole for any other degrees at Universiti Sains Malaysia or other institutions. I grant Universiti Sains Malaysia the right to use the dissertation for teaching, research and promotional purposes.

………………………………
FARAHAMIZAH BINTI OTHMAN

Date: July 2024

ACKNOWLEDGEMENT

Alhamdulillah, I give all praise and glory to Allah, may He grant us all success, for providing me with the strength, knowledge, and patience to complete this thesis. Despite facing numerous hardships and setbacks, I was able to persevere and finish writing this thesis. This thesis would not have been possible without the guidance, support, and encouragement of many individuals. I would like to take this opportunity to express my deepest gratitude to them.

First and foremost, I would like to thank my supervisor, Dr. Mohd Fahmi Mohd Yusoff, for their unwavering support, expert guidance, and invaluable feedback throughout the duration of this project. Their patience and encouragement have been instrumental in the completion of this thesis.

I am also immensely grateful to my co-supervisor, Miss Arifah Nazirah Abdullah, for her insightful comments, constructive criticism, and valuable suggestions that have greatly improved the quality of this work. Her expertise and support have been indispensable.

A special thanks to my field-supervisor, Mr. Ahmad Bazlie bin Abd. Kadir, for his mentorship and for providing me with the practical insights and hands-on experience that were crucial for this research. His dedication and support have been a constant source of motivation.

I would also like to express my sincere appreciation to my friends, Nurul Shazliana binti Mohamad Daud, Nur Syazwany binti Malek, Kong Wei Zhen, and Fatina Ham binti Yahya Ham for their unwavering encouragement, understanding, and for always being there to lift my spirits during challenging times. Their camaraderie and support have made this experience enriching and enjoyable.

Lastly, I owe my deepest gratitude to my family. To my parents, Othman bin Ali and Zainab binti Mohd Shariff, for their unconditional love, support, and sacrifices that have made all of this possible. And to my siblings for their encouragement and belief in me.

This thesis is a testament to the collective efforts of all the individuals. I am deeply grateful for their contributions and support.

Thank you all.

TABLE OF CONTENTS

CERTIFICATE .... **ii**

DECLARATION .... **iii**

ACKNOWLEDGEMENT .... **iv**

TABLE OF CONTENTS .... **v**

LIST OF TABLES .... **vii**

LIST OF FIGURES .... **viii**

LIST OF ABBREVIATIONS .... **ix**

LIST OF APPENDICES .... **x**

STUDY ON NANODOT OSLD IN AIR CAVITY USING ELECTRON BEAM RADIOTHERAPY .... **xi**

ABSTRAK .... **xi**

STUDY ON NANODOT OSLD IN AIR CAVITY USING ELECTRON BEAM RADIOTHERAPY .... **xii**

ABSTRACT .... **xii**

CHAPTER 1 INTRODUCTION **1**

1.1 Background of the study 1

1.2 Problem Statement 2

1.3 Aim of the Study 3

1.4 Specific Objectives of Launching Thesis Template 3

1.5 Significance of study 3

CHAPTER 2 LITERATURE REVIEW **5**

2.1 Electron Beam radiotherapy 5

2.2 Dosimetry in Electron Beam Radiotherapy 6

    2.2.1 Optically Stimulated Luminescence Dosimeter (OSLD) 7

    2.2.2 Utilisation of Nanodot OSLD in Radiotherapy 8

CHAPTER 3 METHODOLOGY 11

3.1 Research Tools 11

3.1.1 OSLD NanoDot 11

3.1.2 OSLD Annealer 12

3.1.3 Microstar InLight Reader 13

3.1.4 Solid Water Phantom 14

3.1.5 Expanded Polysterene (EPS) 16

3.1.6 Markus type Ionization Chamber with Electrometer 17

3.1.7 Linear Accelerator 18

3.1.8 Electron Beam Applicator 19

3.2 Methodology 20

CHAPTER 4 RESULT AND DISCUSSION 22

4.1 Comparison of PDD between OSLD and Ionization Chamber 22

CHAPTER 5 CONCLUSION AND FUTURE RECOMMENDATIONS 27

5.1 Conclusion 27

5.2 Recommendations for Future Research 27

APPENDICES

LIST OF TABLES

Page

Table 4.1 Percentage differences for different thicknesses of air cavity 23

LIST OF FIGURES

Figure 3.1 Nanodot Optically Stimulated Luminescence Detector (OSLD) 12

Figure 3.2 Annealing machine of Nanodot 12

Figure 3.3 MicroStar InLight Reader 13

Figure 3.4 Solid water Phantom 14

Figure 3.5 Expanded Polystyrenes (image courtesy by E&E Foam Manufacturing SDN. BHD) 16

Figure 3.6 Markus type Ionization Chamber with Electrometer 17

Figure 3.7 Linear Accelerator 18

Figure 3.8 Electron Beam Applicator (image courtesy by Nelson Lin, 2018) 19

Figure 3.9 Flowchart of the data collection process 20

Figure 3.10 Arrangement for the depths of data collected 21

Figure 4.1 Graph of PDD for 4cm thickness of air cavities 22

Figure 4.2 Graph of PDD for 6cm thickness of air cavity 22

Figure 4.3 Graph of PDD for 8 cm thickness of air cavity 23

LIST OF ABBREVIATIONS

AAPM	American Association of Physicists in Medicine
CBCT	Cone Beam Computed Tomography
CT	Computed Tomography
EPS	Expanded Polystyrene
HUSM	Hospital Universiti Sains Malaysia
IAEA	International Atomic Energy Agency
ICRU	International Commission on Radiation Units and Measurements
OSLD	Optically Stimulated Luminescence Dosimeter
PDD	Percentage Depth Dose
SSDL	Secondary Standard Dosimetry Laboratory
SSD	Source to Surface distance
VMAT	Volumetric Modulated Arc Therapy
WED	Water Equivalent Depth

LIST OF APPENDICES

Appendix A	TABLE OF RESULTS FOR IONIZATION CHAMBER
Appendix B	TABLE OF RESULTS FOR OSLD

STUDY ON NANODOT OSLD IN AIR CAVITY USING ELECTRON BEAM RADIOTHERAPY

ABSTRAK

Radioterapi sinar elektron dikira bernilai kerana keupayaannya untuk mensasar tisu kanser dengan tepat sambil meminimumkan kerosakan kepada tisu sihat, tetapi ia menghadapi cabaran apabila rongga udara mengganggu taburan dos yang diinginkan. Dosimetri yang tepat adalah penting untuk memastikan dos yang ditetapkan mencapai sasaran sambil menjaga tisu yang sihat. Kajian ini memberi tumpuan kepada menganalisis lengkung Kedalaman Peratusan Dos (PDD) menggunakan dosimeter pendarcahaya rangsangan optik (OSLD) dan membandingkannya dengan pengukuran Kebuk Mengion di bawah ketebalan rongga udara yang berbeza (4 cm, 6 cm, dan 8 cm). Kajian ini menggunakan penggera linear pada 12 MeV, menggunakan fantom air pepejal untuk mensimulasikan tisu dan polisterin digunakan sebagai rongga udara. Pengukuran diambil pada kedalaman yang berbeza untuk menilai bagaimana rongga udara mempengaruhi taburan dos. Hasil kajian menunjukkan perbezaan antara pengukuran OSLD dan Kebuk Mengion, dengan OSLD secara umumnya meramalkan dos, terutamanya di kawasan menaik. Dalam kajian ini, kedua-dua OSLD dan Kebuk Mengion menunjukkan persetujuan yang lebih dekat dalam pengukuran dos di bawah rongga udara, dengan perbezaan 31.7, 12.9, dan 3.1 yang diperhatikan di semua ketebalan rongga. Walau bagaimanapun, kedua-dua kaedah menghadapi kesukaran untuk meramalkan dos dengan tepat di pusat dan permukaan rongga udara.

STUDY ON NANODOT OSLD IN AIR CAVITY USING ELECTRON BEAM RADIOTHERAPY

ABSTRACT

Electron beam radiotherapy is valued for its ability to precisely target cancerous tissues while minimizing damage to healthy ones, but it faces challenges when air cavity disrupts the intended dose distribution. Accurate dosimetry is crucial to ensure the prescribed dose reaches the target while sparing healthy tissues. This research focuses on analyzing Percentage Depth Dose (PDD) curves using Optically Stimulated Luminescent Dosimeters (OSLD) and comparing them with Ionization Chamber measurements under varying air cavity thicknesses (4 cm, 6 cm, and 8 cm). The study utilized a linear accelerator at 12 MeV, employing solid water phantoms to simulate tissue and expanded polystyrene for air cavities. Measurements were taken at different depths to evaluate how air cavities affect dose distribution. The results revealed discrepancies between OSLD and Ionization Chamber measurements, with OSLD generally overestimating the dose, especially in the buildup region. In this study, both Optically Stimulated Luminescent Dosimeters (OSLD) and Ionization Chambers demonstrated closer agreement in dose measurements below the air cavity, with discrepancies of 31.7, 12.9, and 3.1 observed across all cavity thicknesses. However, both methods struggled to accurately estimate doses at the centre and surface of the air cavity.

CHAPTER 1

INTRODUCTION

1.1 Background of the study

Electron beam radiotherapy utilizes high-energy electrons from an electron accelerator to precisely target and treat cancerous tissues, minimizing damage to surrounding healthy areas. These electrons rapidly deposit their energy upon entering the body, achieving 100% dose at a shallow depth before a plateau and subsequent rapid fall-off, with penetration depth depending on the electron beam energy (Icru-35, n.d.).

The effectiveness of this therapy relies on understanding the interactions of electrons with human tissue, including inelastic collisions leading to ionization, excitation, and bremsstrahlung radiation, which affect the electron energy spectrum and treatment precision(Strydom et al., n.d.).

A critical tool in electron beam therapy is the percentage depth dose (PDD) curve, which shows how the dose varies with depth in tissue. Factors like beam energy, field size, and source-to-surface distance influence this curve, allowing clinicians to optimize treatment parameters (“icru-35,” n.d.).

Accurate dose measurement is essential, and various dosimeters are used. Ionization chambers, both cylindrical and parallel-plate, measure depth ionization distribution and convert it to depth dose distribution using the water-to-air stopping power ratio (Gifford, n.d.).

Radiographic and radiochromic films provide visual dose distribution, requiring interpretation via characteristic curves. Optically Stimulated Luminescence

Dosimeters (OSLDs) offer high accuracy and precision, detecting doses as low as 0.1 mGy with ±1% precision. OSLDs are more reliable than thermoluminescent dosimeters (TLDs) for electron beam measurements due to their lower susceptibility to environmental factors like temperature and humidity (Miller, 2024)

1.2 Problem Statement

Air cavities in the human body can significantly affect the dose distribution of electron beams used in radiotherapy. When an electron beam encounters an air cavity, the absence of tissue-equivalent material disrupts the beam's interactions and scattering properties, leading to changes in the dose distribution (Wynand Strydom and Parker, n.d.)(Gifford, n.d.). Specifically, the presence of an air cavity can cause a dose perturbation characterized by an increase in dose at the proximal edge of the cavity and a decrease at the distal edge (Gifford, n.d.). This phenomenon is more pronounced with higher energy electron beams and larger air cavities (Wynand et al., n.d.).

The magnitude of dose perturbation and the degree of lateral electron disequilibrium depend on several factors, including the size and location of the air cavity, the energy of the electron beam, and the field size. Accurate dosimetry becomes crucial in these situations to ensure the intended dose is delivered to the target volume while minimizing exposure to surrounding healthy tissues. Advanced dosimetric techniques, such as Monte Carlo simulations, parallel-plate ionization chambers, and radiochromic films, can be employed to precisely measure and model the dose distribution in the presence of air cavities (Gifford, n.d.)

1.3 Aim of the Study

To analyze the efficiency of OSLD in air cavity for electron beams by using percentage depth dose (PDD).

1.4 Specific Objectives of Launching Thesis Template

i) To compare the PDD in the presence of air cavity using OSLD with and Ionization Chamber.

ii) To evaluate the effect of air cavity thicknesses in OSLD and Ionization Chamber

1.5 Significance of study

This study investigates the impact of air cavities on electron beam radiotherapy using Optically Stimulated Luminescence Dosimeters (OSLD). OSLD technology has proven to be a reliable method for accurately measuring radiation doses across various applications, including research, personal monitoring, and environmental monitoring. However, the role of OSLD technology specifically in the context of air cavities during electron beam therapy has not been extensively explored, and data on this subject are currently lacking. Therefore, this study aims to elucidate the accuracy and efficiency of OSLD in measuring radiation doses within air cavities during electron beam radiotherapy.

The findings of this study could have several significant implications. Firstly, it may contribute to the development of more precise and sensitive techniques for radiation detection. Enhanced accuracy in electron beam therapy treatments can be achieved by providing more reliable data and better understanding the performance of

OSLD in air cavities, ultimately leading to improved patient outcomes. Additionally, this study could assist clinicians and researchers in refining treatment plans and ensuring more effective radiation delivery by offering more accurate data on radiation doses administered in the presence of air cavities.

CHAPTER 2

LITERATURE REVIEW

2.1 Electron Beam radiotherapy

Electron beam radiotherapy leverages the properties of high-energy electrons to effectively target and treat cancerous tissues. These electrons are produced by a sophisticated piece of equipment known as an electron accelerator. Once generated, the electrons are precisely directed toward the tumor, ensuring that the cancer cells receive a concentrated dose of radiation. This targeted approach minimizes damage to surrounding healthy tissues, making it a preferred method for treating certain types of cancer (Icru-35, n.d.)

One of the defining characteristics of electron beam radiotherapy is its dose distribution profile. Upon entering the body, the electrons quickly deposit their energy, reaching 100% of the intended dose at a relatively shallow depth beneath the skin. This is followed by a plateau region where the dose remains relatively uniform. After this uniform region, there is a rapid decrease in the dose, known as the dose fall-off. The specific depths at which these changes occur are determined by the energy of the electron beam: higher energy beams penetrate deeper before the fall-off begins, while lower energy beams have a shallower penetration. (Icru-35, n.d.)

As electrons travel through a medium such as human tissue, they undergo a series of interactions that affect their behavior and energy distribution. These interactions primarily involve inelastic collisions with atomic electrons, leading to ionization and excitation of atoms. Additionally, electrons may collide inelastically with atomic nuclei, resulting in the emission of bremsstrahlung radiation. These processes collectively cause the electrons to lose energy and result in the broadening of their energy spectrum as they penetrate deeper into the tissue. This broadening influences the overall effectiveness and precision of the radiotherapy treatment. (Strydom et al., n.d.)

To accurately understand and utilize electron beam radiotherapy, the percentage depth dose (PDD) curve is a critical tool. The PDD curve represents how the radiation dose varies with depth in the tissue, relative to the maximum dose delivered at the central axis of the beam. The characteristics of this curve are influenced by several factors, including the energy of the electron beam, the size of the field being irradiated, and the distance from the radiation source to the surface of the patient. By analyzing the PDD curve, clinicians can tailor the treatment parameters to maximize the effectiveness of radiation therapy. (Icru-35, n.d.)

2.2 Dosimetry in Electron Beam Radiotherapy

A variety of dosimeters are used to measure the dose distribution of electron beams accurately. One such dosimeter is the ionization chamber. Cylindrical, small-volume ionization chambers are commonly employed to measure the depth ionization distribution of electron beams. These devices are highly precise and reliable, capturing detailed data on ionization levels at various depths. However, the raw ionization measurements must be converted into a depth dose distribution by applying the appropriate stopping power ratios, specifically the water-to-air ratio, at the beam's central axis at a given depth within a phantom. This conversion ensures that the data accurately reflects the dose delivered to the tissue (Gifford, n.d.)

Parallel-plate ionization chambers are another type of dosimeter specifically designed to measure dose distributions in electron beams. Similar to cylindrical ionization chambers, the depth ionization data obtained from parallel-plate chambers must be converted into depth dose distributions. This conversion is done using the water-to-air stopping power ratio, which provides a precise understanding of the dose delivered at various depths. (Gifford, n.d.)

Additionally, radiographic or radiochromic films are utilized to measure dose distributions in electron beams. These films provide a visual representation of dose distribution, with the film density corresponding to the radiation dose received. To interpret the data accurately, the characteristic curve of the specific film used must be applied to determine the dose based on the observed film density (Miller, 2024).

Another advanced dosimeter used for electron beam dosimetry is the optically stimulated luminescence dosimeter (OSLD). OSLDs are renowned for their high accuracy and precision in measuring doses from electron beams. They can detect doses as low as 0.1 mGy with a precision of ±1% or better, making them exceptionally reliable for clinical applications. OSLDs are generally more accurate than thermoluminescent dosimeters (TLDs) for electron beam measurements. This increased accuracy is due to OSLDs' lower susceptibility to environmental factors such as temperature and humidity, which can significantly affect TLD readings (Miller, 2024).

2.2.1 Optically Stimulated Luminescence Dosimeter (OSLD)

Nanodot Optically Stimulated Luminescence Dosimeters (OSLDs) are advanced radiation measurement tools used for precise and reliable dose assessment across various fields, including medical radiation therapy, diagnostic radiology, and radiation protection. These dosimeters offer several advantages, such as their compact size, high sensitivity, and capability for real-time or nearly real-time dose measurements (Musa et al., 2017).

The functioning of nanodot OSLDs is based on the principle of optically stimulated luminescence. When exposed to ionizing radiation, the dosimeter stores energy. Upon subsequent exposure to specific light wavelengths, the dosimeter emits luminescent light proportional to the accumulated radiation dose. This emitted light is then measured to determine the received dose (Retna Ponmalar et al., 2017).

One of the primary advantages of Nanodot OSLDs is their high sensitivity to radiation. They can accurately detect and measure very low doses of ionizing radiation, making them ideal for a wide range of applications, including quality assurance in medical radiation therapy (Retna Ponmalar et al., 2017). Nanodot OSLDs are so tiny and nimble that they resemble tiny buttons or chips. They can be easily positioned in a variety of places thanks to their small size, including inside phantoms or on the skin of patients undergoing medical procedures (Akyol et al., 2019).

Reusable Nanodot OSLDs make dosage measurement more affordable and environmentally friendly. The dosimeter can be "reset" after usage by exposing it to light, which will erase the previous measurement and get it ready for a fresh one. This process is called bleaching (Retna Ponmalar et al., 2017)

2.2.2 Utilisation of Nanodot OSLD in Radiotherapy

Nanodot Optically Stimulated Luminescence Dosimeters (OSLDs) have proven to be invaluable tools in electron beam radiotherapy, offering precise dosimetry and quality assurance across various applications. These dosimeters are extensively utilized for their accuracy, reliability, and compact size, which make them ideal for a range of clinical and research settings

Nanodot OSLDs are particularly effective for measuring surface doses during radiotherapy treatments. Studies have shown that OSLD measurements tend to be higher than those obtained using EBT3 film, especially for 6 MV photon beams. For example, in breast-conserving radiotherapy, OSLD readings ranged from 44.4% to 54.2% of the prescribed dose, whereas EBT3 film measurements were consistently lower by factors of 1.19 and 1.17 for medial and lateral positions, respectively. This highlights the higher sensitivity and accuracy of OSLDs in capturing surface dose variations (Yusof et al., 2015).

The dosimetric properties of Nanodot OSLDs have been extensively characterized for electron beam dosimetry audits. Research indicates that the sensitivity correction factor (SCF) is 1.001 ± 0.25%, with linear dose-response curves for 6 MeV and 9 MeV beams. However, a notable energy dependency was observed at 12 MeV, resulting in a deviation of 4.08% compared to 6 MeV. Additionally, the signal depletion per readout was minimal at 0.03%, and signal fading was 3.20% after 70 days post-irradiation. These characteristics ensure that Nanodot OSLDs provide reliable and consistent measurements over time and across different energy levels (Abdullah et al., 2024).

Nanodot OSLDs are also utilized for in vivo monitoring during total skin electron beam radiotherapy (TSET) treatments. They have demonstrated the ability to accurately measure doses on a patient’s skin during treatments, with results aligning closely with planned doses. Furthermore, OSLDs have been used to assess the necessity for additional shielding or boost fields, proving to be essential for ensuring accurate dose delivery and patient safety in TSET treatments (Kairn et al., 2020).

In clinical settings, Nanodot OSLDs are celebrated for their high accuracy and precision. They are versatile and effective across various applications, including quality assurance and patient treatment monitoring. Their compact size allows for easy positioning in diverse locations, such as within phantoms or on the skin of patients undergoing treatment. The reusability of Nanodot OSLDs, through a process known as bleaching, further enhances their practicality by allowing for cost-effective and environmentally friendly dosage measurements (Kry, 2015.)

CHAPTER 3

METHODOLOGY

3.1 Research Tools

3.1.1 OSLD NanoDot

The Optically Stimulated Luminescence Dosimeters (OSLDs) used in this study were NanoDot dosimeters from Landauer, Inc., Glenwood, IL, as depicted in Figure 1.1. These dosimeters are widely utilized in dosimetry applications. They are composed of aluminium oxide powder doped with carbon, resulting in the chemical formula Al2O3. Each dosimeter is encased in a light-tight housing with dimensions of 10 x 10 x 2 mm^3, ensuring protection from light exposure that could otherwise affect the readings (Akyol et al., 2019).

The calibration and annealing of the OSLDs were performed at the Secondary Standard Dosimetry Laboratory (SSDL) of the Malaysian Nuclear Agency (Nuclear Malaysia). To remove any trapped charge within the OSLDs, they were annealed using high-intensity light from a specialized annealer. Initial readings were taken before any measurements to establish baseline values (Abdullah et al., 2024)

For this study, 57 NanoDot OSLDs were obtained from the SSDL at the Malaysian Nuclear Agency for radiotherapy calibration purposes. Each NanoDot carrier is uniquely identifiable, featuring a 2D barcode on the front and an alphanumeric serial number on the back. These codes are essential for tracking and ensuring the accuracy of each individual OSLD throughout the study.

Figure 3.1 Nanodot Optically Stimulated Luminescence Detector (OSLD)

3.1.2 OSLD Annealer

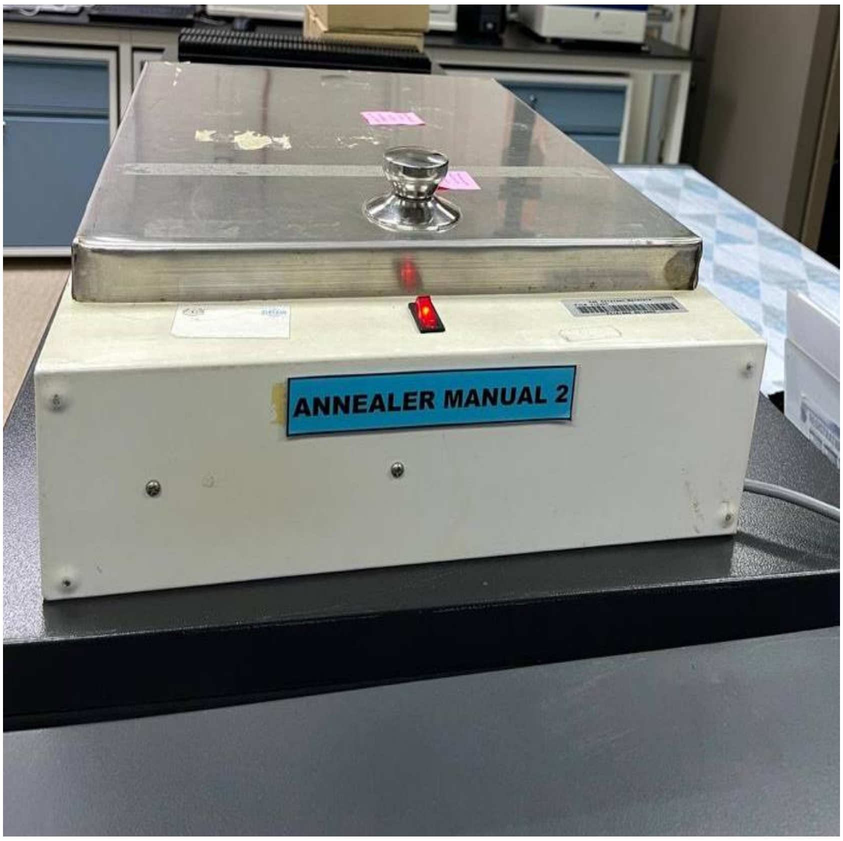

Figure 3.2 Annealing machine of Nanodot

Figure 3.2 illustrates a specialized annealing machine developed by Landauer Inc., specifically designed for NanoDot® dosimeters. Annealing is a vital process in the life cycle of OSLDs, involving the heating of dosimeters to a precise temperature to eliminate any residual radiation signals accumulated during their usage. This procedure effectively resets the dosimeters, ensuring they are ready for accurate radiation measurements in future applications.

The annealing process for NanoDot® dosimeters is notably thorough and time-intensive, taking a significantly longer duration to complete compared to other methods. During this process, each dosimeter is carefully placed within the machine, with a specific arrangement that ensures an adequate distance between them to optimize the annealing efficiency. This meticulous setup is crucial for maintaining the integrity and reliability of the dosimeters' subsequent readings (Saidin et al., 2021).

3.1.3 Microstar InLight Reader

Figure 3.3 MicroStar InLight Reader

The dose readings in this study were performed using the MicroStar InLight reader (Landauer Inc., Glenwood, IL), located at the Malaysian Nuclear Agency. Its design eliminates the need for consumable sources like gas, filters, or heating elements, simplifying setup and operation. The reader is activated by simply plugging it in, making it highly convenient.

The OSLDs are automatically read using a built-in barcode reader, negating the need for pre-analysis sensitivity evaluation. This efficiency, combined with high sensitivity and traceability, makes the MicroStar reader an excellent choice for precise dosimetry.

As shown in Figure 3.3, the MicroStar reader connects to a computer via a USB cable, enabling control, monitoring, setup, analysis, and data recording through the MicroStar software. Its portability allows for immediate on-site analysis, making it ideal for use in confined spaces. The reader provides dose measurements in various units, including mrem, mrad, and cGy, and supports reporting in multiple formats such as XLS, PDF, XML, and CSV. This versatility and ease of use enhance its applicability in diverse dosimetry tasks, ensuring accurate and reliable dose assessments.

3.1.4 Solid Water Phantom

Figure 3.4 Solid water Phantom

The radiotherapy phantom employed in this study is made of Perspex, also known as polymethylmethacrylate (PMMA) with the chemical formula ($C_5H_8O_2$) and a density of 1.185 g/cm³. This material serves as an excellent tissue-equivalent material due to its properties closely mimicking those of human tissue, specifically water. Solid Water® is another plastic compound used in this context, approximating the physical and dosimetric characteristics of soft tissues with similar density, electron density, and stopping power (Butson et al., 2008)

The Perspex slabs used in this study measure 30 x 30 cm² and come in varying thicknesses of 5 cm, 4 cm, 3 cm, 2 cm, and 1 cm, as depicted in Figure 3.4. These slabs are designed to simulate the properties of human tissues, particularly water, which constitutes most soft tissues in the body. To account for backscatter effects, the phantom slabs are placed beneath the radiation detector, ensuring accurate measurement of radiation dose distribution within the tissue-equivalent material.

3.1.5 Expanded Polysterene (EPS)

Figure 3.5 Expanded Polystyrenes (image courtesy by E&E Foam Manufacturing SDN. BHD)

Expanded Polystyrene (EPS) with a density of 10 kg/m³ was employed as a simulation material for air cavities in radiotherapy, as illustrated in Figure 3.5. EPS, known for being lightweight and cost-effective, is increasingly utilized in radiation therapy due to its ability to accurately mimic air cavities and its compatibility with treatment planning systems. Comprising 98% air and only 2% plastic, EPS typically has a physical density ranging from 10 to 30 kg/m³, making it an ideal material for simulating air cavities (EPSOLE, 2024). By choosing an EPS density that closely approximates that of air, more accurate dose calculations and treatment planning in radiotherapy can be achieved.

3.1.6 Markus type Ionization Chamber with Electrometer

Figure 3.6 Markus type Ionization Chamber with Electrometer

The Markus chamber is designed to address the limitations of the Classic Markus chamber, ensuring better energy independence and reduced perturbation effects. It features a thin entrance window made of polyethylene (0.03 mm) and a protective acrylic cover (0.87 mm thick), which provides water equivalence and minimizes radiation scattering. With a small sensitive volume of 0.02 cm^3, the chamber allows for high spatial resolution and precise measurements. Its wide guard ring design further minimizes the influence of scattered radiation from the housing, ensuring perturbation-free measurements. Typically, the chamber is used with an electrometer to measure the ionization current generated by radiation (Pearce, 2004).

3.1.7 Linear Accelerator

Figure 3.7 Linear Accelerator

The data for this research was collected using the Varian Clinac iX linear accelerator (Varian Medical Systems, Palo Alto, CA, USA), as depicted in Figure 3.7. Located in the Radiotherapy Department of Hospital Universiti Sains Malaysia (HUSM), this advanced linear accelerator is primarily used for treatment purposes. The Clinac iX is equipped with 120 multi-leaf collimators (MLC) and includes various components such as a treatment head, patient couch, handheld controller, collimator, kV-on board imager (OBI), cone beam computed tomography (CBCT), and a control panel. These features facilitate a wide range of radiation therapy treatments, including conformal radiation therapy (CRT), intensity-modulated radiation therapy (IMRT), volumetric modulated arc therapy (VMAT), and image-guided radiation therapy (IGRT). The accelerator can deliver photon energies of 6 MV and electron energies of

6, 9, 12, and 15 MeV. For this study, 12 MeV electron beams and a radiation dose of 100 cGy were utilized to irradiate the phantom.

3.1.8 Electron Beam Applicator

Figure 3.8 Electron Beam Applicator (image courtesy by Nelson Lin, 2018)

Electron beam applicators are available in various shapes and sizes, including circular, square, and rectangular forms, to accommodate different treatment field requirements. These applicators are constructed from materials like lead, aluminium, and plastic to minimize radiation leakage and ensure effective shielding. They incorporate scattering foils to evenly distribute the electrons, thereby ensuring a uniform dose distribution within the treatment area. Designed to precisely collimate the electron beam, these applicators focus the radiation on the target area, reducing exposure to surrounding healthy tissues. For shaping irregular fields, collimating blocks made of lead or low-melting point alloys are utilized, providing additional precision in treatment delivery. The applicator used in this research is 15 cm × 15 cm.

3.2 Methodology

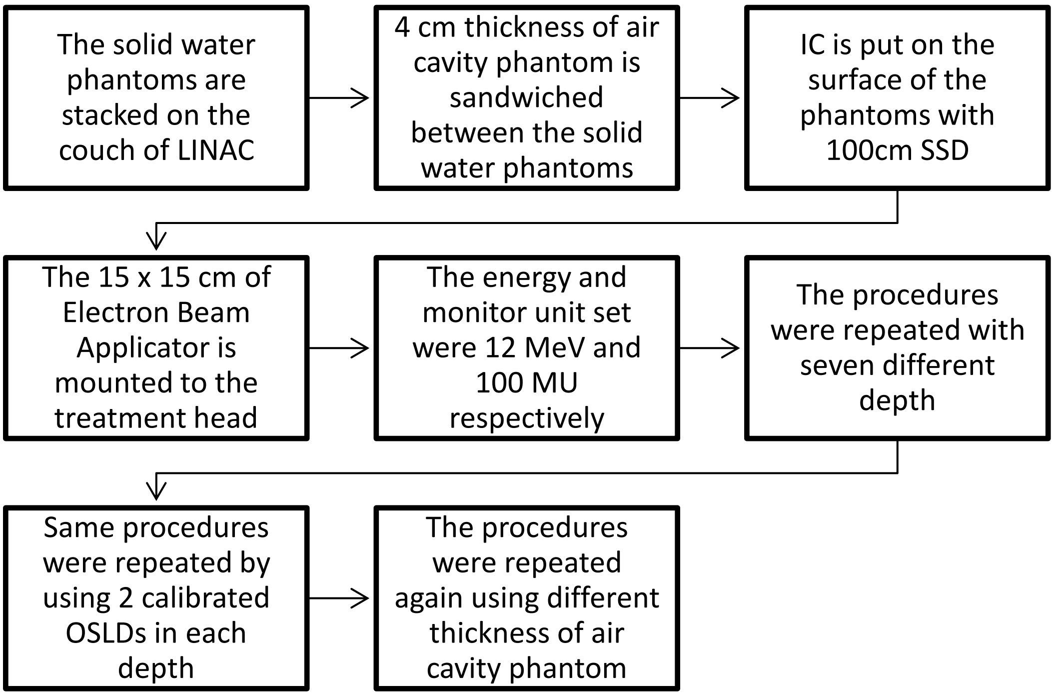

Figure 3.9 Flowchart of the data collection process

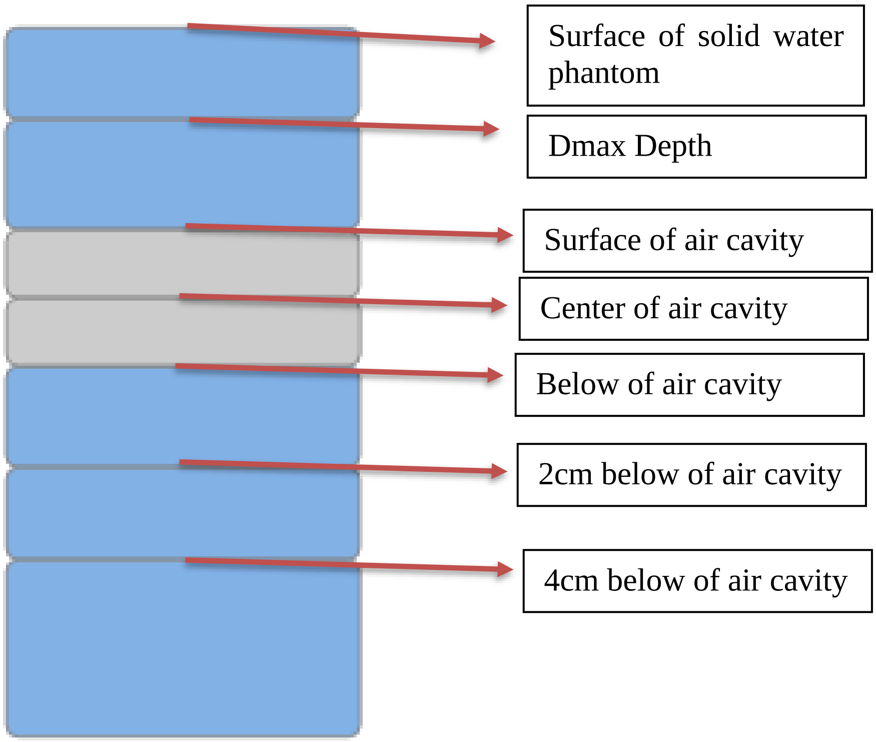

Figure 3.10 Arrangement for the depths of data collected

This study focused on utilizing OSLDs for the dosimetry of 12 MeV electron beams, aiming to compare the results with those obtained from an Ionization Chamber. Specifically, the comparison centered on the Percentage Depth Dose (PDD) data. The research investigated three distinct setups, each featuring air cavities of varying thicknesses: 4 cm, 6 cm, and 8 cm. Dosimetry comparisons were performed across these setups to assess the agreement between OSLDs and the Ionization Chamber regarding PDD measurements. Seven selected depths within the phantom were examined, as illustrated in Figure 3.9.

All measurements were conducted using the Varian Clinax iX linear accelerator with a 12 MeV electron beam, set at a 100 cm Source-to-Surface Distance (SSD) and a field size of 15 cm x 15 cm. To provide clarity, Figure 3.8 illustrates the experimental procedure followed in this study.

CHAPTER 4

RESULT AND DISCUSSION

4.1 Comparison of PDD between OSLD and Ionization Chamber

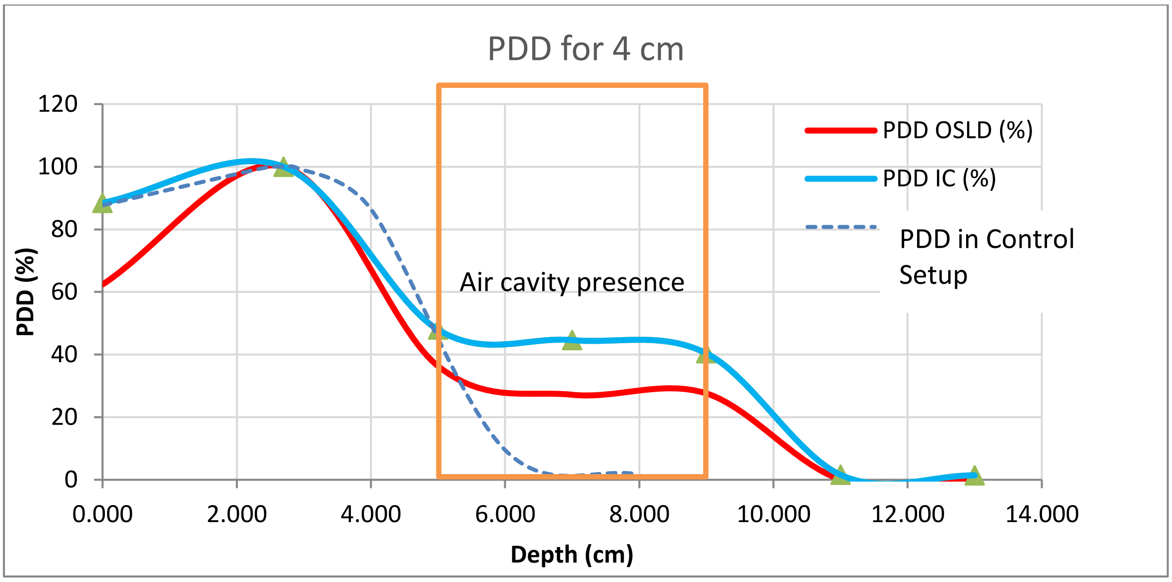

Figure 11 Graph of PDD for 4cm thickness of air cavities

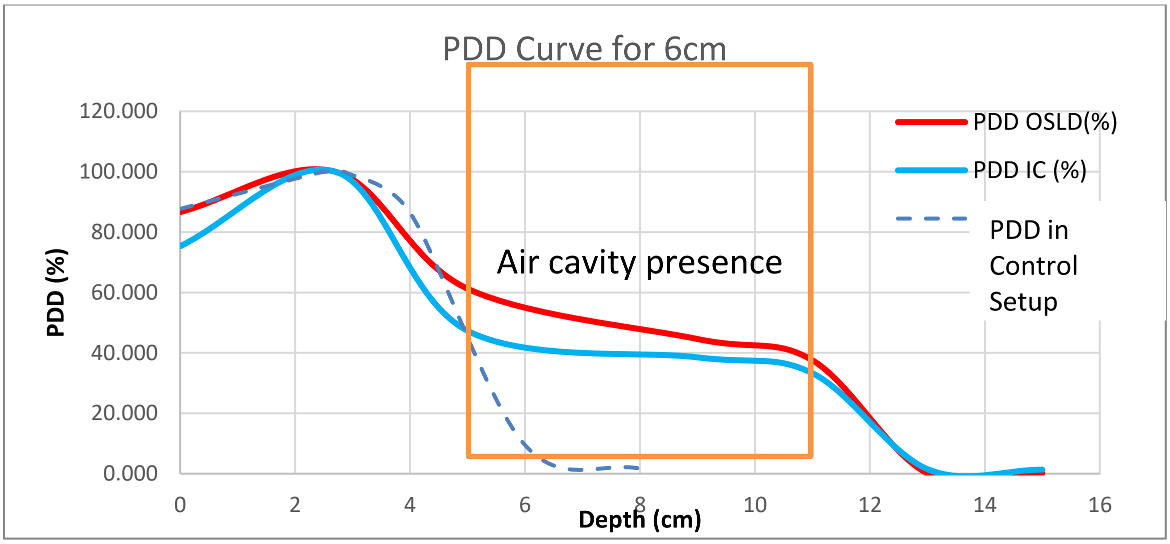

Figure 12 Graph of PDD for 6cm thickness of air cavity

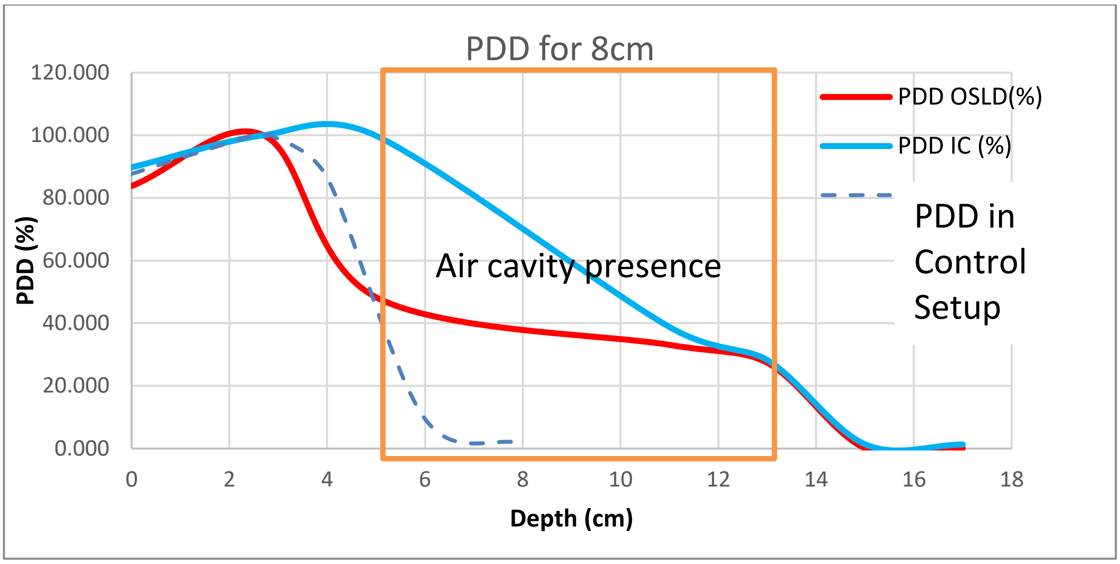

Figure 13 Graph of PDD for 8 cm thickness of air cavity

Table 4.1 Percentage differences for different thicknesses of air cavity

Thickness of air cavity (cm)	Depth (cm)	PDD of Ionization Chamber (%)	PDD of OSLD (%)	Percentage differences (%)
4	Surface	88.444	62.380	29.5
	Dmax	100.000	100.000	0.0
	Surface of air cavity	47.947	36.316	24.3
	Center of air cavity	44.602	27.151	39.1
	Below air cavity	40.395	27.585	31.7
	2cm below air cavity	1.571	0.098	93.8
	2cm below air cavity	1.419	0.085	94.0
6	Surface	75.318	86.642	15.0
	Dmax	100.000	100.000	0.0
	Surface of air cavity	47.328	61.256	29.4
	Center of air cavity	38.524	44.605	15.8
	Below air cavity	33.282	37.568	12.9
	2cm below air cavity	1.527	0.149	90.3
	2cm below air cavity	1.323	0.191	85.5
8	Surface	89.775	83.812	6.6
	Dmax	100.000	100.000	0.0

	Surface of air cavity	99.847	48.298	51.6
	Center of air cavity	38.804	33.098	14.7
	Below air cavity	28.272	27.396	3.1
	2cm below air cavity	1.380	0.133	90.4
	2cm below air cavity	1.278	0.121	90.5